Online Conductivity Calibration Methods for EIT Gas/oil in Water Flow Measurement

Jiabin Jia[2,1], Mi Wang[1,3*], Yousef Faraj[1] and Qiang Wang[1]

[1] School of Chemical and Process Engineering, University of Leeds, Leeds, LS2 9JT, UK
[2] School of Engineering, University of Edinburgh, Edinburgh, EH9 3JL, UK
[3] Sate Key Lab. of O&G Reservoir Geology and Exploitation, Southwest Petroleum University, China

jiabin.jia@ed.ac.uk; m.wang@leeds.ac.uk

ABSTRACT

Electrical Impedance Tomography (EIT) is a fast imaging technique displaying the electrical conductivity contrast of multiphase flow. It is increasingly utilised for industrial process measurement and control. In principle, EIT has to obtain the prior information of homogenous continuous phase in terms of conductivity as a reference benchmark. This reference significantly influences the quality of subsequent multiphase flow measurement. During dynamic industrial process, the conductivity of continuous phase varies due to the effects from the changes of ambient and fluid temperature, ionic concentration, and internal energy conversion in fluid. It is not practical to stop industrial process frequently and measure the conductivity of continuous phase for taking the EIT reference. If without monitoring conductivity of continuous phase, EIT cannot present accurate and useful measurement results. To online calibrate the electrical conductivity of continuous phase and eliminate drift error of EIT measurement, two methods are discussed in this paper. Based on the linear approximation between fluid temperature and conductivity, the first method monitors fluid temperature and indirectly calibrates conductivity. In the second method, a novel conductivity cell is designed. It consists of a gravitational separation chamber with refreshing bypass and grounded shielding plate. The conductivity of continuous phase is directly sensed by the conductivity cell and fed to EIT system for online calibration. Both static and dynamic experiments were conducted to demonstrate the function and accuracy the conductivity cell.

Keywords: EIT, Online conductivity calibration, Flow measurement

1 INTRODUCTION

Electrical Impedance Tomography (EIT) is an imaging technique for the multiphase flow measurement and visualisation. Because EIT is able to provide the cross-sectional images of dispersed phase (gas or oil) in terms of distribution, concentration and velocity, it is increasingly utilised for industrial process measurement and control (York, 2001). The operation procedure of EIT is not complex, particularly for the experiment in laboratory scale. The first step is to take a baseline reference from the conductive continuous phase inside the vessel or pipeline, which is an instant snapshot and only represent the condition of continuous phase (water) in that short moment. These reference data are an array of impedance values measured from the EIT electrodes non-invasively mounted on the internal surface of the experimental vessel or pipeline. Later, dispersed phase (gas/oil) is introduced and mixed with continuous phase in the vessel or pipeline. Each discrete EIT sensing on multiphase mixture is compared with the pervious single set of reference benchmark data. The relative impedance difference between them is utilised to inversely generate the images of multiphase flow using image reconstruction algorithms. The effectiveness of the reference significantly determines the accuracy of EIT measurement. It also raises a challenge for the practical application of EIT to multiphase flow measurement, since the conductivity of continuous phase in industrial process greatly varies due to the effects from the changes of ambient and fluid temperature, ionic concentration, and internal energy conversion in fluid. Without online real-time

conductivity calibration, EIT cannot take the conductivity change of continuous phase into account and will produce large drift error to measurement results. In Sharifi's EIT work, the concentration of solid contents is empirically correlated with temperature, conductivity and composition (Sharifi, 2013). In this paper, the well-known method of calibrating conductivity is reviewed and discussed first. In the contrast, an online conductivity calibration method is introduced to overcome the obstacles restraining the broader industrial application of EIT.

2 TEMPERATURE CALIBRATION

Electrical conductivity indicates the material's capacity of conducting electric current. The electrical conductivity σ of material can be defined as:

$$\sigma = \frac{L}{RA} \tag{1}$$

where R, A and L are the electrical impedance, the cross-sectional area and the length of the material respectively.

The electrical conductivity of electrolyte solution mainly depends on the concentration and composition of ionic species dissolved in the solution. The temperature of electrolyte solution also influences electrical conductivity (Hayashi, 2004). When the temperature change is in the range of 0-30 ºC, the conductivity σ_r at temperature T_r is approximated into a linear relationship as expressed in Equation (2) (Sorensen and Glass, 1987) with respect to initial conductivity σ_0 at temperature T_0 (normally 25 ºC), where k is called temperature coefficient to compensate the effect of temperature on conductivity.

$$\sigma_r = (1 + k(T_r - T_0))\sigma_0 \tag{2}$$

In the case of fluid flow, rearranging Equation (1), $R_0 = L/\sigma_0 A$ is regarded as equivalent impedance of humongous continuous phase at temperature T_0. $R_r = L/\sigma_r A$ is the new impedance after temperature of continuous phase changes to T_r. By combining Equations (1) and (2), the ratio of impedance R_2 and R_1 is denoted in Equation (3), which indicates a linear relation between temperature difference and conductivity ratio of fluid.

$$\frac{R_r}{R_0} = \frac{\sigma_0}{\sigma_r} = \frac{1}{(1 + k(T_r - T_0))} \tag{3}$$

In EIT, sensitivity Back-Projection (SBP) algorithm (Kotre, 1989) is commonly used as image reconstruction method. The derivation from impedance measurement to electrical conductivity is denoted in Equation (4), where S is the sensitivity matrix (Polydorides, 2002), which is the combination of the integrals of dot product between two electric field vector for all the EIT excitation and sensing projection. σ_o is the electrical conductivity of continuous phase and R_r is the impedance of conductive continuous phase. σ_m is the electrical conductivity of multiphase phase mixture and R_m is the impedance of multiphase mixture. Both R_m and R_r are measured using EIT. In author's case, the dimension of the sensitivity matrix S is 316 rows and 104 columns. R_m and R_r are impedance array with 104 elements obtained from EIT measurement, so the relative change of impedance $(R_m-R_r)/R_r$ also is an array with 104 element. The conductivity ratio σ_m/σ_o on the left side of Equation (4) is an array with 316 elements that are data behind the EIT tomographic image.

$$\frac{\sigma_m}{\sigma_0} \approx 1 - S \frac{R_m - R_r}{R_r} \tag{4}$$

In the ideal laboratory scale experiment, to measure R_r, the EIT sensor is filled with the continuous phase (water) first, then the dispersed phase (gas/oil) is introduced to the EIT sensor then measure R_m. It is convenient to get a new R_r by refilling the EIT sensor with continuous phase. However, in the practical industrial production, the homogenous continuous phase may only exist once at the beginning of the process. The initial reference impedance R_0 and temperature T_0 have to be recorded by EIT and temperature sensor. The change of fluid temperature will cause the change of reference impedance. It is difficult to stop the process frequently to create continuous phase only environment for the purpose of taking EIT reference. Rather than updating R_r, T_r is monitored and used for online conductivity calibration as expressed in Equation (5), which is obtained by substituting R_r of Equation (3) into Equation (4).

$$\frac{\sigma_m}{\sigma_0} \approx 1 - S \frac{R_m - (R_0/(1+k(T_r - T_0)))}{R_0/(1+k(T_r - T_0))} \tag{5}$$

To demonstrate the effect of conductivity drift and the significance of conductivity calibration, a test was conducted in a static EIT vessel. The initial reference was taken for EIT at water temperature 23.5 °C. After a rubber plug was placed in the EIT vessel, the tomographic image is shown in Figure 1(a). When the water was heated to 38.4 °C and the rubber plug remained at the same location, the image became Figure 1(b). The plug cannot be recognised anymore in the tomographic image. Unless the conductivity calibration of Equation (5) was applied, Figure 1(b) is restored into Figure 1(c). In this test, the temperature coefficient k is 0.021 and three images have the same colour bar scale.
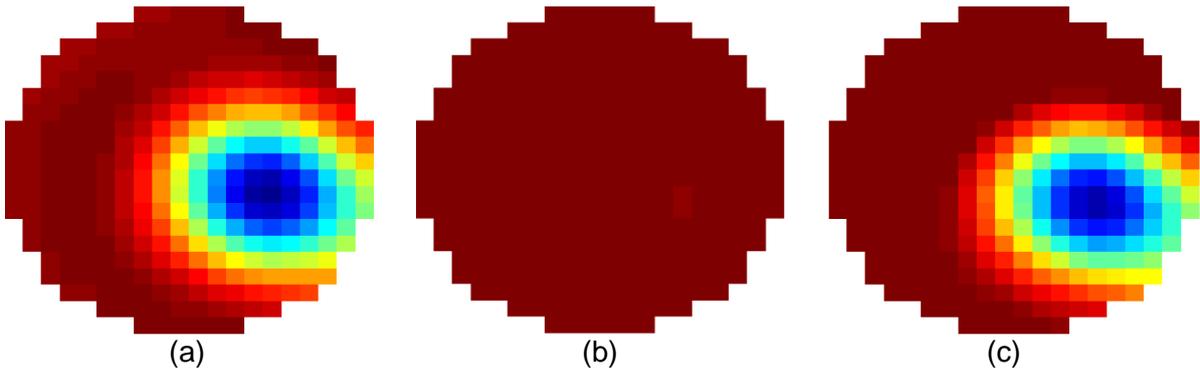

(a) (b) (c)

Figure 1. Conductivity calibration based on temperature
(a) temperature of water 23.5 °C and initial reference (b) temperature of water rises to 38.4 °C with initial reference at 23.5°C (c) after conductivity calibration from temperature

The modified SBP algorithm (Jia, 2015) is another EIT image reconstruction method. The similar steps shown in Equations (6) and (7) could be applied for online conductivity calibration based on temperature.

$$\frac{R_m}{R_r} = (1 + k(T_r - T_0)) \frac{R_m}{R_0} \tag{6}$$

$$\frac{\sigma_m}{\sigma_0} \approx \frac{1}{S \dfrac{R_m}{R_r}} = \frac{1}{S(1 + k(T_r - T_0)) \dfrac{R_m}{R_0}} \tag{7}$$

Monitoring the temperature of fluid flow is a straightforward and indirect calibration method. However, this method has a few drawbacks. First, this method is only suitable if the conductivity change originates from temperature change, rather than from the changes in ionic concentration. Moreover, temperature coefficient k is an empirical parameter fitted from the measurement data. Different electrolyte solution has different temperature coefficient. Finally, when fluid temperature varies over a large temperature range, the linear approximation in Equation (2) is not valid and a nonlinear relationship should apply. Therefore, a better method of calibrating the conductivity change is to directly measure conductivity online. A novel approach is introduced in next section.

3 CONDUCTIVITY CALIBRATION

3.1 Conductivity measurement

In the electrolyte solution, electric current is carried by ions and the electrical conductivity indicates the concentration of ionisable solutes. The principle of conductivity measurement with a tetrapolar configuration is shown in Figure 2. A 10 kHz alternating voltage is applied across electrode 1 and 4 to avoid electrolysis. The consumed current I and the response voltage V are simultaneously sensed across electrode 2 and 3. The conductivity σ is computed using Equation (8) below.

$$\sigma = k\frac{I}{V} \tag{8}$$

where k is a cell constant in unit cm^{-1} and typically in the range of 0.01 cm^{-1} and 50 cm^{-1}. It is affected by the geometry of sensor, i.e. the distance between electrodes and the area of the electrodes. The division of V and I is referred as mutual impedance. The product of mutual impedance and conductivity equals to cell constant k.
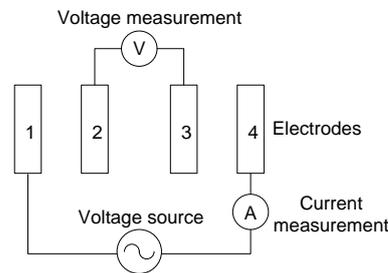

Figure 2. Circuit of conductivity measurement

The conductivity cell is integrated with the EIT system (Jia, 2010) used in the paper. In fact, they have the same measurement mechanism as shown in the circuit of Figure 2. The voltage source is connected across electrode 1 and 4 as driving source. This voltage source can be switched to conductivity cell or EIT electrodes, depending on the measurement object. The benefit of this configuration is that the larger output current can be generated from the voltage source than the conventional current source at 10 kHz frequency region, therefore the amplitude of response voltage across electrode 2 and 3 will not be too weak to be measured accurately. This mechanism can increase the measurement sensitivity of the EIT system and the conductivity cell for highly conductive multiphase flow.

3.2 Design of Conductivity cell

The conductivity of the liquid is directly measured online for real-time conductivity compensation due to the change of ionic concentration or temperature. The assembly of the conductivity cell is illustrated in Figure 3(a). For the applications of concurrent upwards gas-water or oil-water flow, the cell chamber is coupled with a 2 inch pipe section through a 45° downwards pipe fitting. The diameter of the cylinder chamber is 2 inch too. Because each phase has different density, gravitational separation process takes place inside the chamber. Water is accumulated in the lower space of the chamber. The schematic of conductivity cell is enlarged and displayed in Figure 3(b), 4 stainless steel electrodes (4 black spots) are arranged in an equi-spaced fashion and mounted on the bottom of the chamber to directly contact with the liquid in the chamber. To ensure the conductivity of continuous phase in the main flow loop is refreshed rapidly, a flexible flush tube connects the low pressure point along the vertical pipe section and the left bottom corner of the chamber. The water flow rate through the flush tube is controlled by a ball valve. The contained fluid within the chamber is constantly circulated with main flow loop. A curved metal mesh with fine mesh is used to separate of the effective measuring region from fast moving flow and prevent disturbance caused by the other constituent phases. The metal mesh is also connected to the ground of the electronic instrumentation, to ensure air or oil not to contact with any electrodes or close to the measuring region. Two flanges are fixed at either end of the pipe section to facilitate installation of the conductivity spool in any vertical section of a flow line. This conductivity cell could also be used for the inclined loop and horizontal loop but the orientation of the chamber has to be downwards to make sure the fluid full of the chamber. In Figure 3(b), the dotted arrows denote the predicted water flow and solid arrows denote the gas or oil flow. To observe the distribution of gas or oil, Perspex is selected as the material of cell chamber. The valve on the flexible flush tube is controlled to ensure no gas bubbles or oil droplets entering the conductivity sensing area beneath the grounding plate.
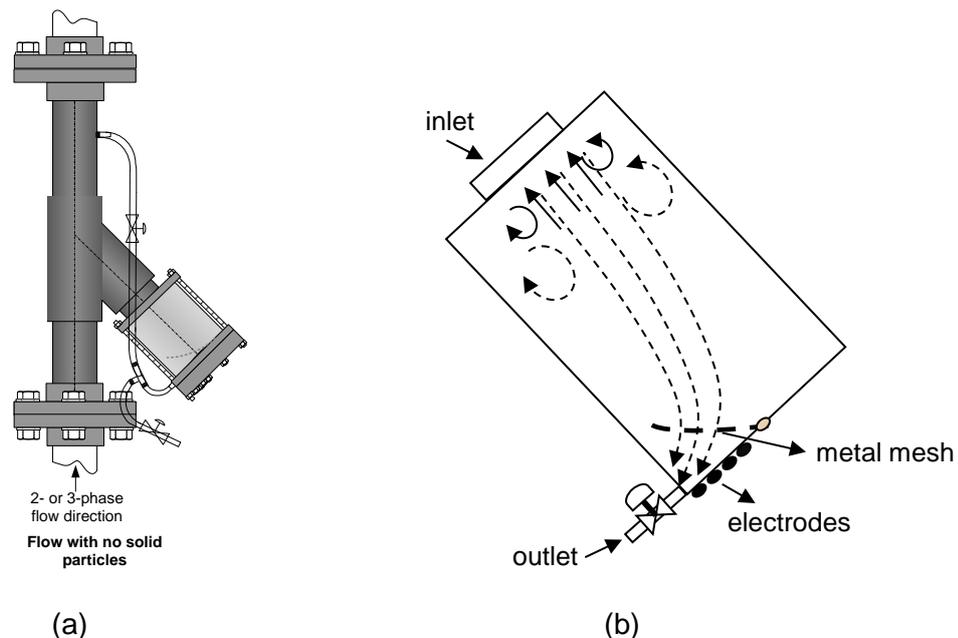

Figure 3. Assembly of the conductivity cell in the flow loop
(a) schematic of conductivity cell, (b) detailed fluid mechanism, the dotted arrows denote the predicted water flow and solid arrow denote the gas or oil flow

3.3 Test of conductivity cell

3.3.1 Static test

To read the value of electrical conductivity from the conductivity cell, the cell constant k in Equation (8) has to be determined first. The aim of this static test is to calibrate the cell constant k against a commercial conductivity probe. Afterwards, the cell constant k is applied to the conductivity cell to measure the conductivity value in S/m. In this test, tap water was heated to 48 °C and poured into the cell chamber. During the natural cooling process, the mutual impedance of the tap water was sensed using the method described in section 3.1, meanwhile, the conductivity of water was recorded from a commercial conductivity probe (Cyberscan PC6500). Figure 4 shows the variation of mutual impedance due to the change of conductivity. Although conductivity and mutual impedance have inverse relationship, within the small range of conductivity (568.7 μS/cm - 664.7 μS/cm), the conductivity and mutual impedance presents a linear relationship approximately. Two dashed straight lines in Figure 4 indicate the ±0.5% error band of the solid linear trend line. According to Equation (8), the product of mutual impedance (V/I) and conductivity (σ) is the cell constant k of the conductivity cell. In Figure 4, 10 products of mutual impedance and conductivity are averaged and the mean cell constant k is determined as 0.064 cm^{-1}.
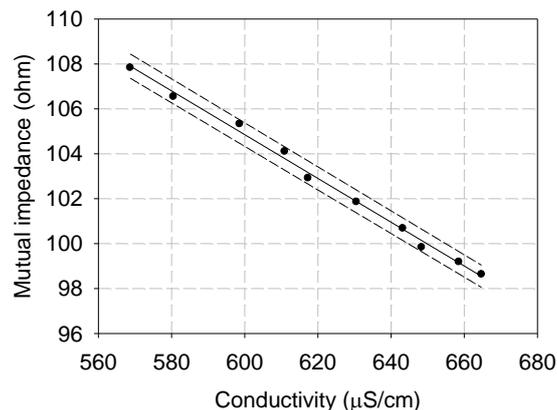

Figure 4. Relationship between mutual impedance and conductivity in static setup

3.3.2 Dynamic test

To test the dynamic response speed of the conductivity cell, the conductivity cell unit was connected in the flow loop at the University of Leeds (Olerni, 2013). In principle, the continuous phase inside the conductivity cell could be rapidly refreshed to indicate the conductivity change of the continuous phase in the main flow loop. To demonstrate the circulation of tap water inside the chamber along the tap water flowing in the loop with 0.73 m^3/hr flow rate. 5 ml blue ink was poured into the tank of the flow loop. The colour of tap water in the flow loop was dyed promptly. Whereas, it took a while for the conductivity cell to be refreshed and have the same colour as tap water in the main flow loop. This test is just a qualitative demonstration of fluid circulation. Another quantitative test was carried out to verify the response speed of the conductivity cell. After 150 g NaCl was added into the water tank, as shown in the black curve in Figure 5, it took 60 second for the conductivity in the water tank to increase and stabilise. The blue curve showed the mutual impedance inside the conductivity cell chamber took approximate 400 second to reach steady state. At current mechanical design, the response time of the conductivity cell to the step conductivity is long. The flow rate of the multiphase flow, the diameter of the flush tube, and height of another end of flush tube will affect the dynamic response speed of the conductivity cell. The refreshing speed is controlled by the valve on the flush tube in the design. Because the appearance of gas/oil phase around the electrodes in the cell can disturb conductivity readings, the priority of the conductivity cell is to ensure the full gravitational separation of different phases within a relevant longer refreshing time. In fact, the temperature change of fluid is a slow process (the temperature of fluid rose

0.47°C per hour in the test) and a sudden change in ionic concentration is not expected in practice, so 400 seconds refreshing time is acceptable.
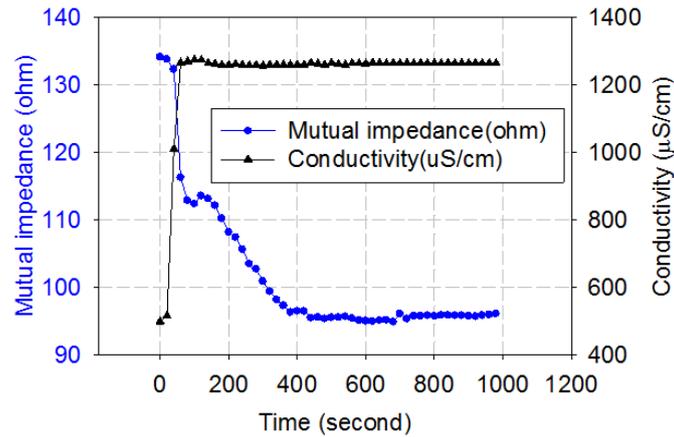

Figure 5. Dynamic response of conductivity cell

The function of conductivity cell was tested in air-water two-phase flow. Water conductivity in the tank was measured using the same commercial conductivity probe mentioned above. The mutual impedance was read from the conductivity cell. The air-water two-phase flow ran for 30 minutes at 0.73 m^3/hr inlet water flow rate and 0.9 m^3/hr inlet air flow rate. During the test, the separation of air and water took place effectively in the chamber and no entrained air bubble was observed. The dynamic energy from the pump was dissipated into heat energy and raised the temperature of the flowing fluid from 22.0 °C to 28.5 °C. Figure 6 does not present as strong linear relationship between mutual impedance and conductivity temperature as Figure 4 in static test. The two dashed lines indicate the ±1% error band of the solid linear trend line, which means the circulation of water inside the separation chamber brings certain disturbance to conductivity measurement. The cell constant k is determined as 0.065 cm^{-1} by averaging 15 cell constant of each individual point in Figure 4.
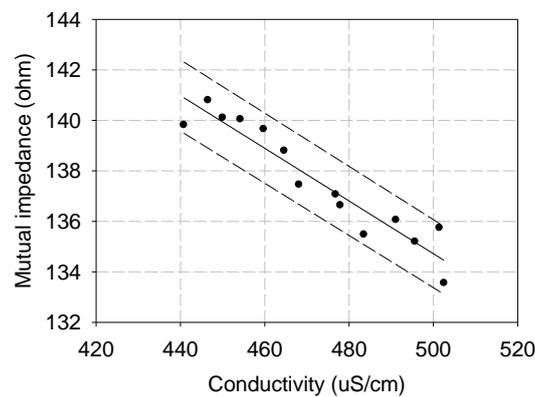

Figure 6. Relationship between mutual impedance and conductivity in dynamic setup

The air-oil-water three-phase flow experiment was carried out at Schlumberger Gould Research (SGR), Cambridge, UK. After 7 hours continuous running, the flow temperature rose from 17.06 °C to 20.32 °C and water conductivity measured from the conductivity cell was monitored accordingly. The inlet flow rate of each phase, flow temperature and water conductivity are listed in Table 1. From the former dynamic test, 0.065 cm^{-1} was adopted as the cell constant in this experiment. The correlation between water continuous phase conductivity and flow temperature is shown in Figure 7. The red dot is regarded as an outlier and ignored. This could be due to low water cut at this particular flow condition, which might

affect the circulation of water in the chamber. The two dashed lines indicate the ±3% error band of solid linear trend line.

Table 1. Conductivity change of air-oil-water three-phase flow

Q_a (m³/hr)	Q_o (m³/hr)	Q_w (m³/hr)	Temperature (°C)	Water conductivity (µS/cm)
2	2	5	17.06	593.3
2	2	10	17.46	608.1
5	2	10	17.93	600.1
15	5	5	18.54	610.2
15	5	10	18.74	614.1
15	2	10	18.86	631.6
20	2	5	18.98	675.7
2	2	5	19.44	632.2
2	2	10	19.89	658.1
5	2	10	20.32	645.5
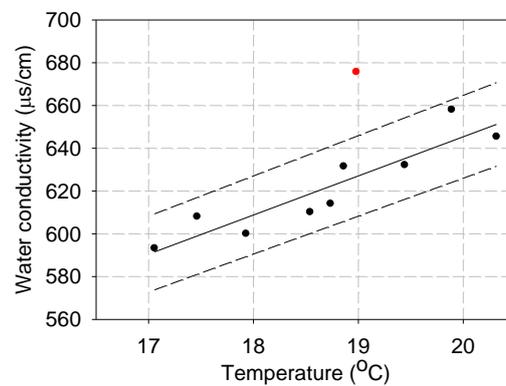
Figure 7. Relationship between temperature and conductivity in dynamic setup

As the oil density is much closer to that of water, the separation of oil and water in the chamber may not be as efficient as that of air and water. Figure 8 shows the photograph of the chamber, which was taken during a three-phase testing in SGR. By observing the chamber, it can be noticed that some oil droplets segregated on the internal wall of the cylindrical chamber. The concerns were raised, as to these oil droplets may be the source of contributing error, which affects the accuracy of the measured conductivity. The water cut against water conductivity is plotted in Figure 9. There is no evident correlation demonstrated between two variables, which indicates that the conductivity cell functions well within the water cut range used in SGR experiment.
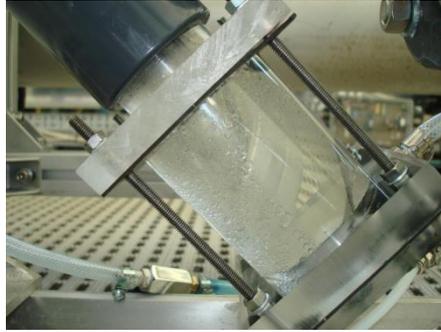
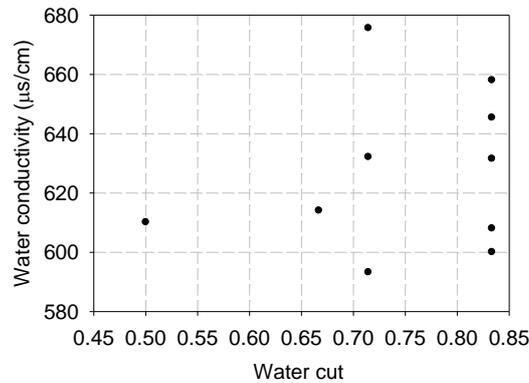**Figure 8.** Oil droplets segregate on the internal wall of the cell chamber

Fig**ure 9.** Correlation between water cut and water conductivity

4 CONCLUSIONS

In the industrial process of multiphase flow, the electrical conductivity of continuous phase fluctuates, which severely deteriorates the performance of EIT measurement, unless the conductivity of continuous phase is constantly monitored and online conductivity calibration is deployed. Detecting the fluid temperature then deriving the corresponding conductivity is a simple approach, however, this calibration method is suitable if the variation of conductivity is caused only by the change of temperature and cannot be applied for the conductivity calibration, due to changes in the ionic concentration or both temperature and ionic concentration. A novel conductivity cell structure is designed to directly online measure the conductivity of continuous phase in the multiphase flow. In the cell chamber, each phase is separated by the different density and water phase was circulated along the main flow loop and conductivity is sampled. The experimental results demonstrate a reasonably good performance of the conductivity cell for air-water two-phase flow and air-oil-water three-phase flow. Two objectives will be focused for future study. (1) Optimise the response time of the conductivity cell meanwhile keep efficient phase separation in the chamber. (2) Test the function of conductivity cell when the conductivity change caused by ionic concentration of continuous phase.

ACKNOWLEDGMENTS

REFERENCES

HAYASHI, M., (2004), Temperature-Electrical Conductivity Relation of Water for Environmental Monitoring and Geophysical Data Inversion*, Environmental Monitoring and Assessment*, 96(1-3), pp. 119-128.

JIA, J., WANG, M., SCHLABERG, H.I. and LI, H. (2010) A novel tomographic sensing system for high electrically conductive multiphase flow measurement, *Flow Measurement and Instrumentation*, 21(3), pp. 184-190.

JIA, J., WANG, M. and FARAJ, Y. (2015) Evaluation of EIT systems and algorithms for handling full void fraction range in two-phase flow measurement, *Measurement Science and Technology*, 26(1), pp.1-7.

KOTRE, C. J., (1989), A sensitivity coefficient method for the reconstruction of electrical impedance tomograms, *Clinical Physics and Physiological Measurement*, 10, pp. 275-281.

OLERNI, C., JIA, J. and WANG, M. (2013) Measurement of Air Distribution and Void Fraction of an Upward Air-water Flow Using Electrical Resistance Tomography and Wire-mesh Sensor, *Measurement Science and Technology*, 24(3), pp.1-9.

POLYDORIDES, N. (2002) Image Reconstruction Algorithms for Soft-Field Tomography: *PhD Thesis* University of Manchester Institute of Science and Technology, UK

SHARIFI, M and YOUNG B., (2013) Towards an online milk concentration sensor using ERT: Correlation of conductivity, temperature and composition, Journal of Food Engineering, 116(1), pp. 86-96.

SORENSEN, J. A. and GLASS, G. E. (1987), Ion and temperature dependence of electrical conductance for natural waters, Analyt. Chem. 59, pp.1594−1597.

YORK, T. (2001) Status of electrical tomography in industrial applications, Journal of Electronic Imaging, 10(3), pp. 608-619.